

# Systematic description of ${}^6\text{Li}(n, n') {}^6\text{Li}^* \rightarrow d + \alpha$ reactions with the microscopic coupled-channels method

T. Matsumoto,<sup>1,\*</sup> D. Ichinkhorloo,<sup>2</sup> Y. Hirabayashi,<sup>3</sup> K. Katō,<sup>2</sup> and S. Chiba<sup>4</sup>

<sup>1</sup>*Meme Media Laboratory, Hokkaido University, Sapporo 060-8628, Japan*

<sup>2</sup>*Division of Physics, Graduate School of Science, Hokkaido University, Sapporo 060-0810, Japan*

<sup>3</sup>*Information Initiative Center, Hokkaido University, Sapporo 060-0810, Japan*

<sup>4</sup>*Japan Atomic Energy Agency (JAEA), Tokai, Naka, Ibaraki 319-1195, Japan*

(Dated: November 11, 2018)

We investigate  ${}^6\text{Li}(n, n') {}^6\text{Li}^* \rightarrow d + \alpha$  reactions by using the continuum-discretized coupled-channels method with the complex Jeukenne-Lejeune-Mahaux effective nucleon-nucleon interaction. In this study, the  ${}^6\text{Li}$  nucleus is described as a  $d + \alpha$  cluster model. The calculated elastic cross sections for incident energies between 7.47 and 24.0 MeV are in good agreement with experimental data. Furthermore, we show the neutron spectra to  ${}^6\text{Li}$  breakup states measured at selected angular points and incident energies can be also reproduced systematically.

PACS numbers: 24.10.Eq, 25.40.Fq

## I. INTRODUCTION

The  ${}^6\text{Li}$  nucleus is known to have a well developed  $d + \alpha$  cluster structure and the binding energy is very small 1.47 MeV from the  $d + \alpha$  breakup threshold. Because of those features, a breakup process of  ${}^6\text{Li}$  into  $d$  and  $\alpha$  is one of the significant mechanisms of the reaction, and the accurate description is required. As one of the most reliable methods for treating breakup processes, the continuum-discretized coupled channels (CDCC) method [1] has been proposed and successfully applied to analyses of three-body breakup systems, in which the projectile breaks up into two constituents, such as  ${}^6\text{Li}$  into  $d$  and  $\alpha$ . Thus, the CDCC method is expected to be indispensable to analyze  ${}^6\text{Li}$  breakup reactions.

For the CDCC analyses of  ${}^6\text{Li}$  elastic and inelastic scattering on various targets, Sakuragi *et al.* [2] have suggested to reproduce the absolute values of a lot of experimental data of cross sections very well. They have also resolved the anomalous renormalization problem [3] in folding model potentials of  ${}^6\text{Li}$  by showing large dynamical polarization potentials due to breakup processes. Furthermore the CDCC method has been also applied to the sequential Coulomb/nuclear breakup via the resonance state of  ${}^6\text{Li}$ , in which both Coulomb and nuclear breakup processes were taken into account consistently [4]. The Coulomb breakup is of a great interest as the time-reversed reaction of the radiative capture reaction,  $d + \alpha \rightarrow {}^6\text{Li} + \gamma$ , which is one of a key reaction in the nucleosynthesis in the early Universe or during stellar evolution [5]. So, it is important that the method could describe not only the nuclear breakup process but also the Coulomb breakup one on an equal theoretical footing. In spite of their efforts, the CDCC method has not been confirmed yet its applicability to breakup to continuum states of  ${}^6\text{Li}$ , especially breakup spectra of  ${}^6\text{Li}$ . This is a basic interest of the theoretical framework to describe reaction mechanisms relevant to breakup processes.

The  $n + {}^6\text{Li}$  reactions are important not only from the basic research interest as shown above but also from the application point of view. Lithium isotopes will be used as a tritium-breeding material in  $d-t$  fusion reactors, and accurate nuclear data are required for  $n$ - and  $p$ -induced reactions. Indeed, IAEA is organizing a research coordination meeting to prepare nuclear data libraries for advanced fusion devices, FENDL-3, and the maximum incident energy is set at 150 MeV to comply fully with the requirements for the IFMIF design [6]. Lithium isotopes are ones of important materials in these libraries. As a matter of fact, the neutron interaction with lithium and associated breakup reactions are indispensable in determining the neutron energy spectra in blankets of fusion reactors. Thus the tritium breeding ratio, nuclear heating distributions and radiation damage of structural materials are affected by the  $n + \text{Li}$  reactions significantly.

In spite of the importance of the  $n + {}^6\text{Li}$  reaction as described above, experimental data leading to  ${}^6\text{Li}$  continuum breakup processes are extremely rare for the neutron energy region above 20 MeV [7–9]. Furthermore, the statistical model, used often in evaluation of nuclear data for medium to heavy nuclei, cannot be applied to the  ${}^6\text{Li}(n, n')$  reactions. As mentioned in Refs. [10, 11], the mechanisms leading to three- or four-body final states,  $n + d + \alpha$  and  $n + n + p + \alpha$ , are important. Therefore more reliable theoretical calculations for the cross sections are highly desirable.

In this paper, cross sections for  ${}^6\text{Li}(n, n') {}^6\text{Li}^* \rightarrow d + \alpha$  reactions are evaluated by using the microscopic coupled-channels method [2, 12], in which we adopt microscopic wave functions of  ${}^6\text{Li}$  with the  $d + \alpha$  model and the complex Jeukenne-Lejeune-Mahaux effective nucleon-nucleon (JLM) interaction [13] between  $n$  and  ${}^6\text{Li}$ . The calculated elastic, inelastic cross sections and continuum neutron spectra to  ${}^6\text{Li}$  breakup states show good agreement with the experimental data at low neutron incident energies, where breakup effects of  ${}^6\text{Li}$  into  $d$  and  $\alpha$  are dominant. Furthermore we discuss applicability of the approach used here to the present system for the neutron energy region up to 150 MeV.

This paper is organized as follows. In Sec. II, we describe

\*Electronic address: tmatsumoto@nucl.sci.hokudai.ac.jp

the CDCC method including calculations of  ${}^6\text{Li}$  wave functions and coupling potentials with the JLM interaction. In Sec. III and Sec. IV, we present the calculated results and discuss the applicability, respectively. Finally, we give a summary in Sec. V.

## II. FORMULATION

The  $n + {}^6\text{Li}$  scattering system is described as a  $n + d + \alpha$  three-body model, and the Schrödinger equation is written by

$$\left[ K_R + \sum_{j \in {}^6\text{Li}} v_{j0} + H_{6\text{Li}} - E \right] \Psi(\boldsymbol{\xi}, \mathbf{R}) = 0, \quad (1)$$

where  $\mathbf{R}$  and  $\boldsymbol{\xi}$  represent a coordinate between  $n$  and the center-of-mass of  ${}^6\text{Li}$  and a set of internal coordinates of  ${}^6\text{Li}$ , respectively.  $K_R$  is a kinetic energy operator associated with  $\mathbf{R}$ ,  $H_{6\text{Li}}$  is the internal Hamiltonian of  ${}^6\text{Li}$ , and an effective interaction between  $j$ th nucleon in  ${}^6\text{Li}$  and  $n$  is represented by  $v_{j0}$ .

The total wave function with the total angular momentum  $J$  and its projection  $M$  on  $z$ -axis,  $\Psi_{JM}$ , is expanded in terms of the orthonormal set of eigenstates of  $H_{6\text{Li}}$ . Here, microscopic wave functions of  ${}^6\text{Li}$  based on the  $d$ - $\alpha$  cluster model are written as

$$\Phi_\ell^{Im}(\boldsymbol{\xi}) = \psi_\ell^{Im}(\mathbf{r})\varphi(\alpha)\varphi(d), \quad (2)$$

where  $\mathbf{r}$  is the relative coordinate between  $d$  and  $\alpha$ . The  $d$ - $\alpha$  relative wave function with the angular momentum  $\ell$ , total spin  $I$  and its projection  $m$  on  $z$ -axis,  $\psi_\ell^{Im}$ , can be described as

$$\psi_\ell^{Im}(\mathbf{r}) = \phi_\ell^I(r) [i^\ell Y_\ell(\Omega_r) \otimes \eta_d]_{Im}, \quad (3)$$

with the spin of deuteron,  $\eta_d = 1$ . The internal ground state wave functions of  $d$  and  $\alpha$ ,  $\varphi(d)$  and  $\varphi(\alpha)$ , are assumed as inert core. In the present calculation, we use the same internal model Hamiltonian of the  $d$ - $\alpha$  system,  $H_{6\text{Li}}$ , adopted in Ref. [2], which are fixed to reproduce the experimental data of the ground state (-1.47 MeV) and  $3^+$ -resonance state (0.71 MeV) as well as low-energy part of  $d$ - $\alpha$  scattering phase shifts. The ground state is assumed to be a pure  $S$  state ( $\ell = 0$ ), and the calculated wave functions well reproduce not only the elastic electron scattering form factor but also the inelastic one to the  $3^+$ -resonance state [2]. In this framework, we take into account the totally antisymmetrized effect by assuming the orthogonal condition model [14].

In the CDCC method, the relative wave functions of  ${}^6\text{Li}$  for the ground and continuum states are described as a finite number of discretized states denoted by

$$\hat{\psi}_{i\ell}^{Im}(\mathbf{r}) = \hat{\phi}_{i\ell}^I(r) [i^\ell Y_\ell(\Omega_r) \otimes \eta_d]_{Im} \quad (i = 0-N), \quad (4)$$

whose energies  $\epsilon_{i\ell}^I$  are given by

$$\epsilon_{i\ell}^I = \langle \hat{\psi}_{i\ell}^{Im}(\mathbf{r}) | H_{6\text{Li}} | \hat{\psi}_{i\ell}^{Im}(\mathbf{r}) \rangle. \quad (5)$$

As the discretization approach, we adopt the pseudo-state method [15–17] here. The advantage of the pseudostate method is that if there are resonances in its excitation spectrum, we can describe discretized continuum states with a reasonable number of the basis functions, without distinguishing the resonance states from non-resonant continuous states as mentioned in Ref. [16]. As well known,  ${}^6\text{Li}$  has three resonances in  $\ell = 2$ . Therefore the pseudostate method is very useful for analyses of  ${}^6\text{Li}$  breakup reactions.

In the pseudostate method, we diagonalize  $H_{6\text{Li}}$  in a space spanned by a finite number of  $L^2$ -type basis functions for  $r$ ,  $\{\varphi_{j\ell}\}$ , and discretized wave functions for the radial part,  $\{\hat{\phi}_{i\ell}^I\}$  are obtained by

$$\hat{\phi}_{i\ell}^I(r) = \sum_{j=1}^{j_{\max}} A_{j\ell}^I \varphi_{j\ell}(r). \quad (6)$$

As the basis functions, the complex-range Gaussian basis functions [16, 18] are adopted, and we include  $\ell = 0$  and 2 for the relative angular momentum of  $d$ - $\alpha$ :  ${}^1S$  represents the  $S$ -wave state with  $I = 1$ , and  ${}^1D$ ,  ${}^2D$ , and  ${}^3D$  correspond to the  $D$ -wave state with  $I = 1, 2$ , and 3, respectively. The number of states  $N$  is decided as involving all open channels for each incident energy.

After the discretization and the truncation of  $d$ - $\alpha$  continuum,  $\Psi_{JM}$  is reduced to an approximate one,

$$\begin{aligned} \Psi_{JM}^{\text{CDCC}} &= \sum_L \mathcal{Y}_{JM}^{01L} \hat{\phi}_{00}^1(r) \hat{\chi}_{\gamma_0}(\hat{P}_{\gamma_0}, R) / R \\ &+ \sum_{i=1}^N \sum_{\ell} \sum_I \sum_L \mathcal{Y}_{JM}^{\ell I L} \hat{\phi}_{i\ell}^I(r) \hat{\chi}_{\gamma}(\hat{P}_{\gamma}, R) / R, \end{aligned} \quad (7)$$

with

$$\mathcal{Y}_{JM}^{\ell I L} = [[i^\ell Y_\ell(\Omega_r) \otimes \eta_d]_I \otimes i^L Y_L(\Omega_R)]_{JM} \varphi(\alpha) \varphi(d), \quad (8)$$

where  $\gamma_0 = (0, 0, 1, L, J)$  and  $\gamma = (i, \ell, I, L, J)$  represent the elastic channel and breakup channels, respectively. The expansion-coefficient  $\hat{\chi}_{\gamma}$  in Eq. (7) represents the relative motion between  $n$  and  ${}^6\text{Li}$ , and  $L$  is the orbital angular momentum regarding  $\mathbf{R}$ . The relative momentum  $P_{\gamma}$  is determined by the conservation of the total energy,

$$E = \hat{P}_{\gamma}^2 / 2\mu + \epsilon_{i\ell}^I, \quad (9)$$

with  $\mu$  the reduced mass of the  $n + {}^6\text{Li}$  system. Multiplying Eq. (1) by  $[\hat{\phi}_{i\ell}^I(r) \mathcal{Y}_{JM}^{\ell I L}]^*$  from left, one can obtain a set of coupled differential equations for  $\hat{\chi}_{\gamma}$ , called the CDCC equation. Solving the CDCC equation under the appropriate asymptotic boundary condition, we can obtain the elastic and discrete breakup  $S$ -matrix elements. Details of the formalism of the CDCC method are shown in Ref. [1].

For the calculation of diagonal and coupling potentials in the CDCC equation, we use the complex Jeukennd-Lejeune-Mahaux effective nucleon-nucleon (JLM) interaction [13] based on a single folding model. The JLM interaction can be easily applied to coupled-channels calculations of nucleon-nucleus systems, such as Refs. [12, 19]. This interaction has

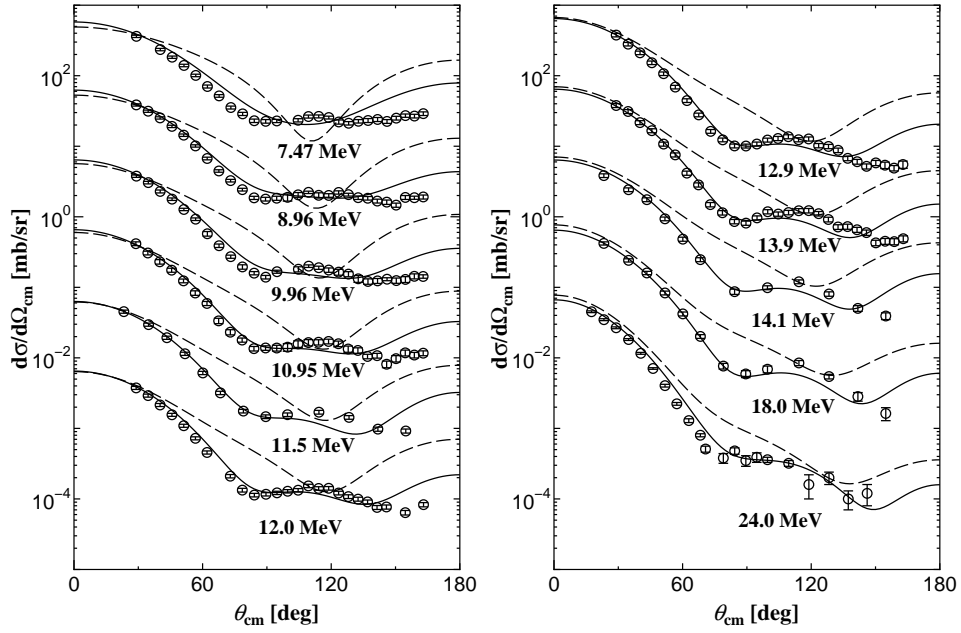


FIG. 1: Angular distribution of the elastic differential cross section of  $n + {}^6\text{Li}$  scattering for incident energies between 7.47 and 24.0 MeV. The solid and dashed lines correspond to the result with and without couplings to breakup states of  ${}^6\text{Li}$ , respectively. Experimental data are taken from Refs. [8–10]. The data are subsequently shifted downward by a factor of  $10^{-1}$ - $10^{-5}$  from 8.96 MeV to 12.0 MeV on the left panel, and  $10^{-1}$ - $10^{-4}$  from 13.9 MeV to 24.0 MeV on the right panel, respectively.

energy and density dependence, and forms a Gaussian with both real and imaginary parts;

$$v_{j0}(R_{j0}; \rho, E) = \lambda_v V(\rho, E) \exp(-R_{j0}/t_R^2) + i\lambda_w W(\rho, E) \exp(-R_{j0}/t_I^2), \quad (10)$$

where  $R_{j0}$  is a coordinate of a nucleon in  ${}^6\text{Li}$  and  $n$ . The parameters,  $t_R$ ,  $t_I$ , and  $\lambda_v$ , are taken as the same ones used in the original paper [13],  $t_R = t_I = 1.2$  and  $\lambda_v = 1.0$ . Meanwhile the normalization for the imaginary part,  $\lambda_w$ , is optimized to reproduce the elastic cross sections, because the strength corresponding to the loss of flux depends on the model space considered in the calculation. Details for strengths of  $V(\rho, E)$  and  $W(\rho, E)$  are shown in Ref. [13].

Using the JLM interaction, the diagonal and coupling potentials,  $V_{\gamma\gamma'}$ , are obtained by

$$V_{\gamma\gamma'}(R) = \int \rho_{\gamma\gamma'}(\mathbf{s}, \Omega_R) v_{j0}(E, \bar{\rho}, \mathbf{R}_{j0}) d\mathbf{s} d\Omega_R, \quad (11)$$

where transition densities,  $\rho_{\gamma\gamma'}$ , and averaged matter density,  $\bar{\rho}$ , of  ${}^6\text{Li}$  between  $\gamma$  and  $\gamma'$  are defined by

$$\rho_{\gamma\gamma'}(\mathbf{s}, \Omega_R) = \langle \mathcal{Y}_{JM}^{iLL} \hat{\phi}_{i\ell}^I | \sum_{j \in {}^6\text{Li}} \delta(\mathbf{s} - \mathbf{s}_j) | \mathcal{Y}_{JM}^{i'L'L'} \hat{\phi}_{i'\ell'}^{I'} \rangle \xi, \quad (12)$$

and

$$\bar{\rho}(s) = \frac{1}{2} \int \{ \rho_{\gamma\gamma}(\mathbf{s}, \Omega_R) + \rho_{\gamma'\gamma'}(\mathbf{s}, \Omega_R) \} d\Omega_s d\Omega_R, \quad (13)$$

respectively. Here  $\mathbf{s}_j$  is a coordinate of  $j$ th particle in  ${}^6\text{Li}$  relative to the center-of-mass of  ${}^6\text{Li}$ .

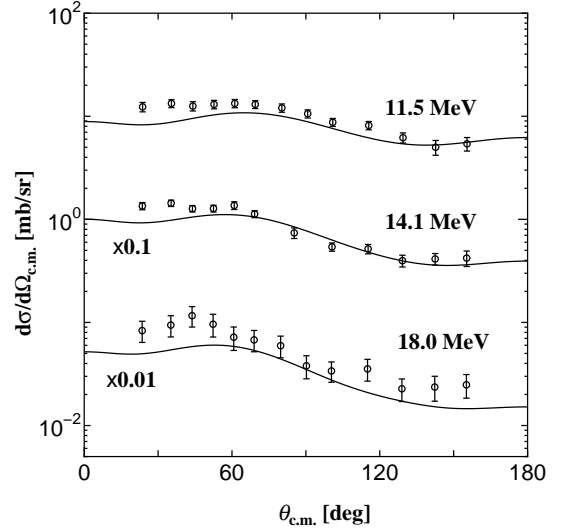


FIG. 2: Neutron inelastic scattering angular distribution to the  $3^+$ -resonance state 0.71 MeV above the  $d$ - $\alpha$  threshold. The experimental data are taken from Ref. [10]. The data for 14.1 (18.0) MeV are shifted by a factor of 0.1 (0.01).

### III. RESULTS

Figure 1 shows the differential elastic cross sections of  $n + {}^6\text{Li}$  for incident energies between 7.47 and 24.0 MeV. One sees that the results of the CDCC calculation represented by the solid lines are in good agreement with the experimental

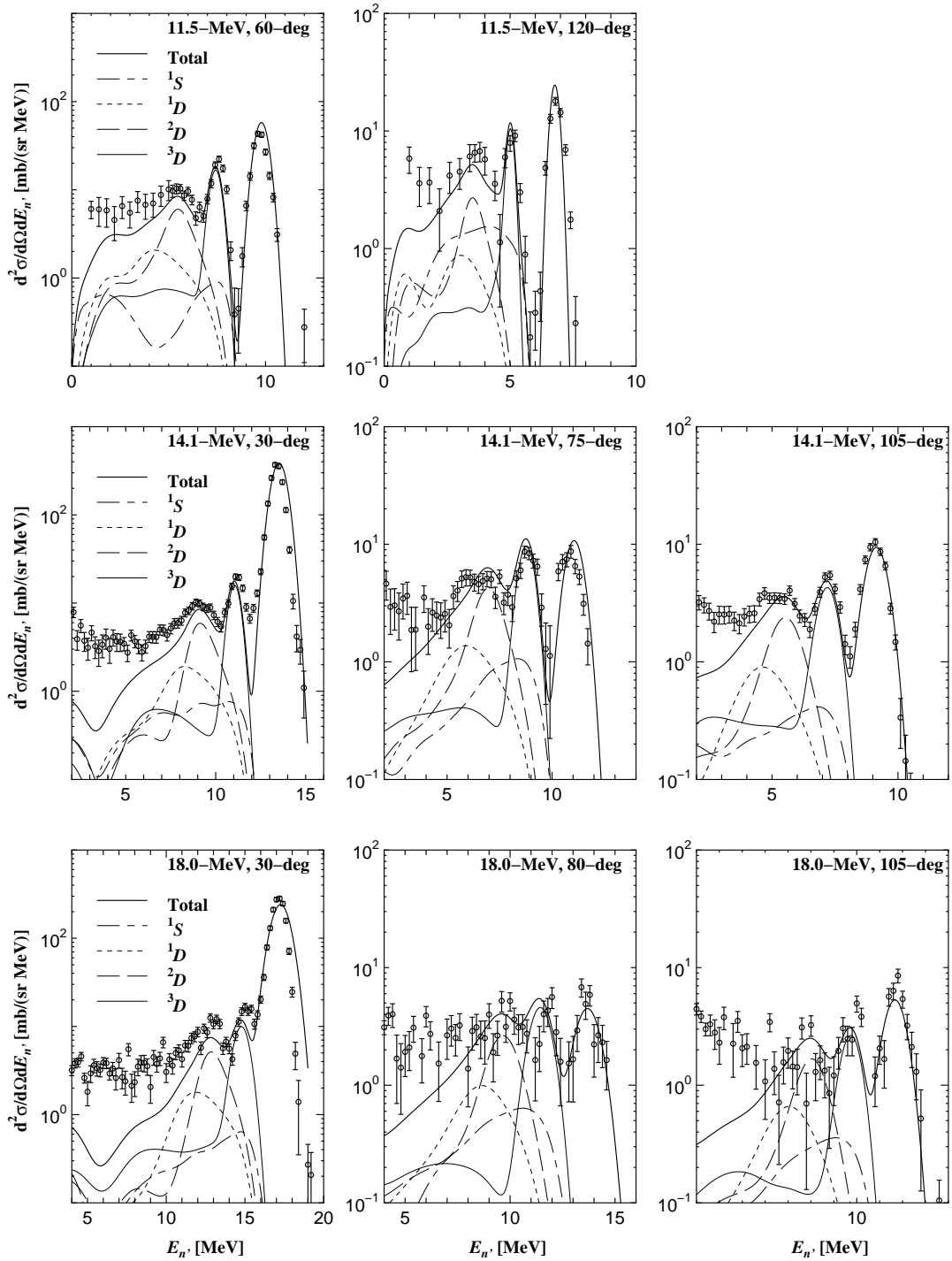


FIG. 3: The neutron spectra calculated by the CDCC method with the JLM interaction comparing with measured data at selected angular points in the laboratory system. The experimental data are taken from Ref. [10].

data. The dashed lines represent results of a single channel calculation, in which couplings to breakup states are omitted. It is found that breakup effects shown by the difference between the dashed and solid lines are significant to reproduce the angular distributions of the elastic scattering. For all incident energies, we take  $\lambda_w = 0.1$  to reproduce the data. The

main component of the flux loss from the elastic channel is due to breakups of  ${}^6\text{Li}$  to  $d$  and  $\alpha$ , which can be taken into account in the CDCC calculation directly. The other effects of the flux loss, such as the excitation of  $\alpha$  and  $d$  breakup, are not so large because of low incident energies. Therefore the strength of  $\lambda_w$  becomes very small. Here, it should be

noted that the single channel calculation cannot reproduce the experimental data if any values of  $\lambda_w$  are taken.

Figure 2 shows the angular distributions to the first excited  $3^+$  state of  ${}^6\text{Li}$  for  $E_n = 11.5, 14.1,$  and  $18.0$  MeV. The theoretical cross sections are calculated by integrating the breakup cross section to  $3^+$ -continuum for the resonance energy region. One sees that the CDCC calculation can also reproduce the inelastic cross section.

In Fig. 3, the calculated neutron spectra are compared with the experimental data at selected angles in the laboratory frame and incident energies. Components of  ${}^1S, {}^1D, {}^2D,$  and  ${}^3D$  are represented by the dash-dotted, dashed, dotted and thin solid lines, respectively, and these results are broadened by considering the finite resolution of the experimental apparatus [10]. Three peaks in the experimental data represent the elastic, inelastic to the  $3^+$ -resonance, and  $2^+$ -resonance components, respectively, from higher neutron energies. The CDCC calculation gives a good agreement with experimental data at the higher neutron energy region. On the other hand in the low neutron energy region, which corresponds to high excited states of  ${}^6\text{Li}$ , the calculated cross section underestimates the experimental data for all energies and angles. The result indicates that experimental data contain contribution from the  $(n, 2n)$  reaction corresponding to a four-body breakup reaction  ${}^6\text{Li}(n, nnp)\alpha$ , as mentioned in Ref. [10]. In the present calculation, the four-body breakup effect is not taken into account directly, and the effect is treated as a absorption effect on the elastic cross section.

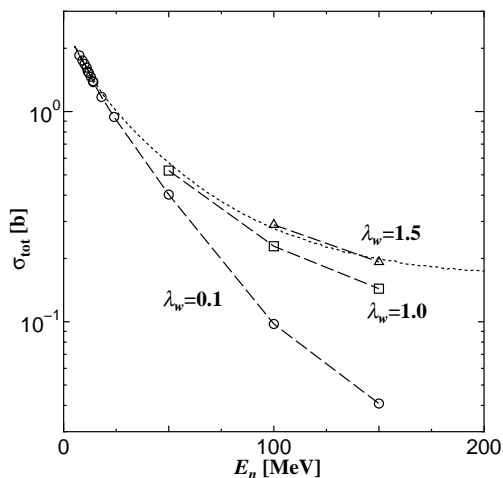


FIG. 4: Neutron energy dependence of the total cross section of  $n + {}^6\text{Li}$  scattering. The dotted line represents the experimental data [20]. The open circles, squares, and triangles corresponds to results with  $\lambda_w = 0.1, 1.0,$  and  $1.5,$  respectively.

#### IV. DISCUSSION

Theoretically the CDCC calculation with the JLM interaction can estimate cross sections of the  $n + {}^6\text{Li}$  scattering for neutron energies up to 160 MeV, which is the maximum applicable energy suggested in the original paper [13]. However for

higher incident energies ( $> 30$  MeV) there is no experimental data of the elastic cross section, which are needed to optimize the normalization factor of the imaginary part. One of the optimization methods is to fit the neutron total cross section data of  ${}^6\text{Li}$ , which have been measured up to 560 MeV [20]. Figure 4 shows the measured total cross section comparing with the calculated ones with  $\lambda_w = 0.1, 1.0,$  and  $1.5$  represented by open circles, squares, and triangles, respectively. One sees that large values for  $\lambda_w$  are required with respect to increasing the neutron energy. Although the energy dependence for  $\lambda_w$  is rationalized because absorption effects become strong as increasing the energy, the optimized value at 150 MeV is much large about  $\lambda_w = 1.5$ . This normalization problem would be resolved by analyzing  $p + {}^6\text{Li}$  elastic cross sections, which have been measured at higher incident energies, within the present framework. Furthermore for higher incident neutron energies four-body breakup effects of  ${}^6\text{Li}(n, nnp)\alpha$  are not negligible. Therefore we require the four-body CDCC calculation, which has been successful for analyses of  ${}^6\text{He}$  breakup reactions [21–25], in the higher energy region.

#### V. SUMMARY

We analyze  ${}^6\text{Li}(n, n'){}^6\text{Li}^* \rightarrow d + \alpha$  reactions by using the continuum-discretized coupled-channels method with the complex Jeukenne-Lejeune-Mahaux effective nucleon-nucleon interaction. In the present analysis, it is found that the elastic cross sections for incident energies between 7.47 and 24.0 MeV can be reproduced by the present analysis with one normalization parameter for the imaginary part of the JLM interaction ( $\lambda_w = 0.1$ ), and breakup effects on the elastic cross section are significant. Furthermore the calculated inelastic cross section to the  $3^+$ -resonance state and neutron spectra are also good agreement with the experimental data systematically. Thus, the CDCC method with the JLM interaction is expected to be indispensable for the data evaluation of the  ${}^6\text{Li}(n, n')$  reactions, and the advantage is to obtain not only elastic and inelastic cross sections but also neutron spectra within the same framework.

For higher neutron incident energies, we have also discussed the applicability of the present microscopic approach. It is found that the required normalization factor  $\lambda_w$  is much large,  $\lambda_w = 1.5$  for 150 MeV, from the analyses of the total cross section. In order to investigate the normalization problem we should analyze  $p + {}^6\text{Li}$  elastic scattering, which have been measured at higher incident energies. Furthermore the four-body CDCC calculation is required to describe the four-body breakup process of  ${}^6\text{Li}$  into  $n + p + \alpha$ , which becomes significant for the higher energy. These results will be reported in a forthcoming paper.

#### Acknowledgments

We would like to thank the members of Nuclear Theory Group at Hokkaido University. This work was supported by JSPS AA Science Platform Program.

- 
- [1] M. Kamimura, M. Yahiro, Y. Iseri, Y. Sakuragi, H. Kameyama and M. Kawai, *Prog. Theor. Phys. Suppl.* **89**, 1 (1986); M. Yahiro, N. Nakano, Y. Iseri and M. Kamimura, *Prog. Theor. Phys.* **67**, 1467 (1982).
- [2] Y. Sakuragi, M. Yahiro and M. Kamimura, *Prog. Theor. Phys.* **89**, 136 (1986); Y. Sakuragi, M. Yahiro, and M. Kamimura, *Prog. Theor. Phys.* **70**, 1047 (1983).
- [3] G. R. Satchler and W. G. Love, *Phys. Rep.* **55**, 183 (1979).
- [4] Y. Hirabayashi and Y. Sakuragi, *Phys. Rev. Lett.* **69**, 1892 (1992).
- [5] W. A. Fowler, *Rev. Mod. Phys.* **56**, 149 (1984).
- [6] "Fusion Evaluated Nuclear Data Library FENDL 3.0", IAEA (<http://www-nds.iaea.org/fendl3/>).
- [7] S. Chiba, et al., *Phys. Rev. C* **58**, 2205(1998) 5.
- [8] H.H. Hogue, P.L. von Hehren, D.W. Glasgow, S.G. Glendinning, P.W. Lisowski, C.E. Nelson, F.O. Purser, W. Tornow, C.R. Gould, and L.W. Seagondollar, *Nucl. Sci. Eng.* **69**, 22 (1979).
- [9] L.F. Hansen, J. Rapaport, X. Wang, F.A. Barrios, F. Petrovich, A.W.Carpenter, and M.J.Threapleton, *Phys. Rev. C* **38**, 525 (1988).
- [10] S. Chiba, T. Fukahori, K. Shibata, B. Yu, and K. Kosako, *Fusion Eng. Des.* **37**, 175 (1997)
- [11] T. Fukahori, S. Chiba, N. Kishida, M. Kawai, Y. Oyama, and A. Hasegawa, Status of JENDL Intermediate Energy Nuclear Data, Proceedings of the International Conference on Nuclear Data for Science and Technology, Trieste, Italy, 1997 (Societa Italiana di fisica, (1997), p. 899
- [12] M. Takashina, and Y. Kanada-En'yo, *Phys. Rev. C* **77**, 014604 (2008).
- [13] J.-P. Jeukenne, A. Lejeune, and C. Mahaux, *Phys. Rev. C* **16**, 80 (1977).
- [14] S. Saito, *Prog. Theor. Phys.* **41**, 705 (1969).
- [15] A. M. Moro, J. M. Arias, J. Gómez-Camacho, I. Martel, F. Pérez-Bernal, R. Crespo and F. Nunes, *Phys. Rev. C* **65**, 011602(R) (2001).
- [16] T. Matsumoto, T. Kamizato, K. Ogata, Y. Iseri, E. Hiyama, M. Kamimura, and M. Yahiro, *Phys. Rev. C* **68**, 064607 (2003).
- [17] T. Egami, K. Ogata, T. Matsumoto, Y. Iseri, M. Kamimura, and M. Yahiro, *Phys. Rev. C* **70**, 047604 (2004).
- [18] E. Hiyama, Y. Kino and M. Kamimura, *Prog. Part. Nucl. Phys.* **51**, 223 (2003).
- [19] N. Keeley, and V. Lapoux, *Phys. Rev. C* **77**, 014605 (2008).
- [20] W. P. Abfalterer, F. B. Bateman, F. S. Dietrich, R. W. Finlay, R. C. Haight, and G. L. Morgan, *Phys. Rev. C* **63**, 044608 (2001).
- [21] T. Matsumoto, E. Hiyama, K. Ogata, Y. Iseri, M. Kamimura, S. Chiba, and M. Yahiro, *Phys. Rev. C* **70**, 061601(R) (2004).
- [22] T. Matsumoto, T. Egami, K. Ogata, Y. Iseri, M. Kamimura, and M. Yahiro, *Phys. Rev. C* **73**, 051602(R) (2006).
- [23] M. Rodríguez-Gallardo, J. M. Arias, J. Gómez-Camacho, R. C. Johnson, A. M. Moro, I. J. Thompson, and J. A. Tostevin, *Phys. Rev. C* **77**, 064609 (2008).
- [24] M. Rodríguez-Gallardo, J. M. Arias, J. Gómez-Camacho, A. M. Moro, I. J. Thompson, and J. A. Tostevin, *Phys. Rev. C* **80**, 051601(R) (2009).
- [25] T. Matsumoto, K. Katō, and M. Yahiro, *Phys. Rev. C* **82**, 051602(R) (2010).